

Sr₄M₃ReO₁₂ (M = Co, Fe): New Ferromagnetic Perovskite Oxides

Abanti Nag,[†] J. Manjanna,[‡] R. M. Tiwari,[†] and J. Gopalakrishnan^{*†}

Solid State and Structural Chemistry Unit, Indian Institute of Science, Bangalore 560012, India, and NDE and Science Research Center, Faculty of Engineering, Iwate University, Morioka 020-8551, Japan

Received March 14, 2008. Revised Manuscript Received April 25, 2008

We describe the synthesis, structure, and magnetic properties of two new perovskite oxides, Sr₄M₃ReO₁₂ (M = Co, Fe), that exhibit ferromagnetism with fairly high ordering temperatures ($T_c = \sim 250\text{--}300$ K). While the M = Co phase crystallizes in a partially ordered double perovskite ($Fm\bar{3}m$) structure ($a = 7.8153$ Å), the M = Fe phase adopts a primitive cubic perovskite ($Pm\bar{3}m$) structure ($a = 3.9353$ Å), where the transition metal atoms are not ordered in the long range. Magnetization studies revealed bulk ferromagnetism for both oxides, but the disordered structures seem to preclude a long-range magnetic order and a definite T_c . While further studies are needed to establish the exact origin of magnetism of these materials, the present investigation reveals the possibility of designing new ferromagnetic oxides based on $M^{3+}\text{--O--Re}^{7+}$ (M = Co, Fe) magnetic interaction in the perovskite related structures.

Introduction

Ferromagnetic perovskite oxides have attracted attention^{1,2} since the discovery of room temperature tunneling magnetoresistance and half-metallicity in the ordered double perovskite³ Sr₂FeMoO₆, the prime motivation being the search for new magnetic materials for application in spintronics—spin-based electronics.⁴ Among the large number of ordered double perovskites A₂MM'O₆ (A are alkaline earth metals, and M and M' are transition metals) that are known,⁵ only a handful of them containing specific combinations of M and M' atoms, such as Fe/Mo, Fe/Re, Cr/Re, and Cr/W, exhibit both ferromagnetic and half-metallic character,¹ revealing stringent requirements in terms of the electronic structure for the occurrence of desired magnetic and metallic properties. In chemical terms, this requirement manifests as mixed valency (valence degeneracy) for specific combinations of M (Fe^{3+/2+}, Cr^{3+/2+}) and M' (Mo^{6+/5+}, Re^{6+/5+}, W^{6+/5+}) atoms, as originally envisaged by Sleight and Weiher.⁶ The presence of M and M' atoms in valence states that are not normally stable under ambient conditions places stringent limitations on the synthesis of these double perovskites; accordingly, synthesis has to be carried out in closed tubes^{7,8} and/or in reducing conditions⁹ with the appropriate control of oxygen partial pressure to ensure

required oxygen stoichiometry/valence control of M and M' atoms in A₂MM'O₆. We believed that it should be possible to realize new ferromagnetic perovskite oxides with combinations of M and M' atoms having air-stable oxidation states, which would obviate the need for working in closed tube/reducing conditions. For this purpose, we chose to explore Re⁷⁺/M³⁺ (M = Mn, Fe, Co, Ni) combinations in perovskite (AMO₃) oxides, keeping in mind that these oxidation states are not only air-stable but also that their (aqueous solution) reduction potentials¹⁰ (Re⁷⁺/Re⁶⁺: 0.72 V; Fe⁶⁺/Fe³⁺: 0.81 V; and Co⁴⁺/Co³⁺: 0.70 V) are favorable for the occurrence of mixed valence states (Re^{7+/6+}, Fe^{3+/4+}, Co^{3+/4+}) in perovskite oxides. Inasmuch as electropositive alkaline earth atoms at the A site of the perovskite structure can stabilize high oxidation states for the M site atoms, we explored the formation of perovskite oxides of the composition A₄M₃ReO₁₂ for A as Ca, Sr, and Ba and M as Mn, Fe, Co, and Ni. Our investigations resulted in the synthesis of two new perovskite oxides, Sr₄M₃ReO₁₂ (M = Co, Fe), that exhibit a high temperature ferromagnetism. The details of synthesis, structure, and magnetic and electrical properties of these two oxides are described in this paper.

Experimental Procedures

The formation of perovskite oxides for the composition A₄M₃ReO₁₂ for A as Ca, Sr, and Ba and M as Mn, Fe, Co, and Ni were explored by reacting stoichiometric mixtures of the starting materials [high purity ACO₃, MC₂O₄·2H₂O, and Re₂O₇ (predried at 120 °C)] at elevated temperatures (900–1200 °C) in air for varying durations. Perovskite formation was found only for two compositions: Sr₄Co₃ReO₁₂ and Sr₄Fe₃ReO₁₂. Single phase products

* Corresponding author. E-mail: gopal@sscu.iisc.ernet.in; tel.: 91-80-2293 2537; fax: 91-80-2360 1310.

[†] Indian Institute of Science.

[‡] Iwate University.

- (1) Serrate, D.; De Teresa, J. M.; Ibarra, M. R. *J. Phys.: Condens. Matter* **2007**, *19*, 23201.
- (2) Goodenough, J. B. *Rep. Prog. Phys.* **2004**, *67*, 1915.
- (3) Kobayashi, K.-I.; Kimura, T.; Sawada, H.; Terakura, K.; Tokura, Y. *Nature (London, U.K.)* **1998**, *395*, 677.
- (4) Felser, C.; Fecher, G. H.; Balke, B. *Angew. Chem., Int. Ed.* **2007**, *46*, 668.
- (5) Anderson, M. T.; Greenwood, K. B.; Taylor, G. A.; Poeppelmeier, K. R. *Prog. Solid State Chem.* **1993**, *22*, 197.
- (6) Sleight, A. W.; Weiher, J. F. *J. Phys. Chem. Solids* **1972**, *33*, 679.
- (7) Gopalakrishnan, J.; Chattopadhyay, A.; Ogale, S. B.; Venkatesan, T.; Greene, R. L.; Millis, A. J.; Ramesha, K.; Hannoyer, B.; Marest, G. *Phys. Rev. B: Condens. Matter Mater. Phys.* **2000**, *62*, 9538.

- (8) Kato, H.; Okuda, T.; Okimoto, Y.; Tomioka, Y.; Oikawa, K.; Kamiyama, T.; Tokura, Y. *Phys. Rev. B: Condens. Matter Mater. Phys.* **2004**, *69*, 184412.

- (9) Huang, Y. H.; Lindén, J.; Yamauchi, H.; Karppinen, M. *Chem. Mater.* **2004**, *16*, 4337.

- (10) Shriver, D. F.; Atkins, P. W. *Inorganic Chemistry*, 3rd ed.; Oxford University Press: New York, 1999; Appendix 2.

of the latter were obtained by reacting stoichiometric mixtures of the reactants at 1200 °C (for Co)/1100 °C (for Fe) with repeated grinding and heating several times.

The products were examined by scanning electron microscopy (SEM), energy dispersive X-ray analysis (EDX), and powder X-ray diffraction (XRD). A JEOL JSM 5600 LV microscope fitted with a Link/ISIS system from Oxford Instruments was used for SEM and EDX analyses. A Philips X'Pert diffractometer (Ni filtered Cu K α radiation) was used to record powder XRD patterns. Lattice parameters were obtained by least-squares refinement of powder XRD data by means of the program PROSZKI,¹¹ and XRD patterns were simulated by the program POWDERCELL.¹² Oxygen stoichiometry of the samples was determined by thermogravimetry (TG) under hydrogen reduction (1H₂/1Ar gas mixture, 40 mL/min) on a Cahn TG-131 system, at a heating rate of 3 °C/min. Typically, hydrogen reduction occurred according to the following chemical reaction: Sr₄M₃ReO₁₂ + 8H₂ = 4SrO + 3M + Re + 8H₂O.

For structure refinement, XRD data were collected in the 2 θ range of 3–100° with a step size of 0.02° and a step time of 9 s using a Philips X'Pert diffractometer (Cu K α radiation). Rietveld refinement of powder XRD data was carried out with the program GSAS.¹³ The patterns were refined for lattice parameters, scale factor, background (shifted Chebyshev background function), pseudo-Voigt profile function (*U*, *V*, *W*, and *X*), atomic coordinates, and isothermal temperature factors (*B*_{iso}).

Magnetic measurements were carried out using a superconducting quantum interference device (SQUID) magnetometer, Quantum Design MPMS-XL. Magnetization (*M*) was measured under zero-field-cooled (ZFC) and field-cooled (FC) configurations as a function of temperature and/or applied field (*H*). The dc electrical resistivity measurements were carried out in the temperature range of 50–300 K on sintered pellets using the standard four-probe method that employs an Advantest R6144 as the current source and an Agilent 34420A multimeter.

Results and Discussion

Among the several A₄M₃ReO₁₂ (*A* = Ca, Sr, and Ba, and *M* = Mn, Fe, Co, and Ni) compositions investigated, perovskite oxides were formed only for Sr₄M₃ReO₁₂ (*M* = Co, Fe). SEM and EDX analyses of the latter samples (Supporting Information) showed that they were single phases (particle size of 3–15 μ m) having the expected metal atom ratios, within the limits of experimental error. TG weight losses under hydrogen reduction (Supporting Information) showed that the samples were oxygen stoichiometric, Sr₄M₃ReO₁₂, indicating formal oxidation states of M³⁺ and Re⁷⁺ for the transition metals.

Powder XRD patterns (Figures 1 and 2) show that both Sr₄M₃ReO₁₂ (*M* = Co, Fe) possess perovskite-based structures, all the prominent reflections being indexable on the basis of a cubic perovskite subcell of *a*_p = ~3.92 Å. For the *M* = Co phase, additional supercell reflections are clearly seen, suggesting the formation of an ordered superstructure. We could readily index all the reflections on a double perovskite cell with *a*_d \approx 2*a*_p = 7.8153 Å. The powder

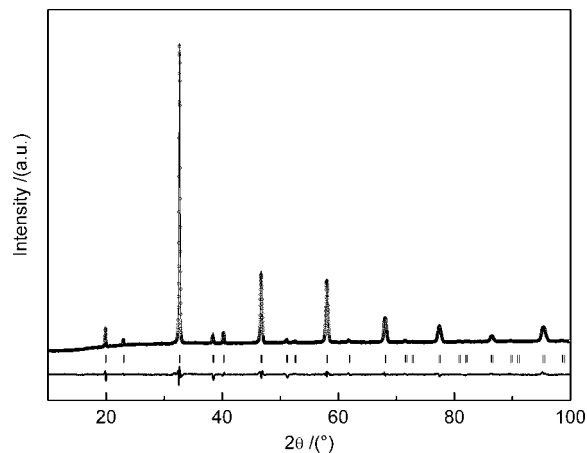


Figure 1. Rietveld refinement of structure of Sr₄Co₃ReO₁₂ from powder XRD data. Observed (○), calculated (—), and difference profiles (bottom) are shown. Vertical bars indicate positions of Bragg reflections.

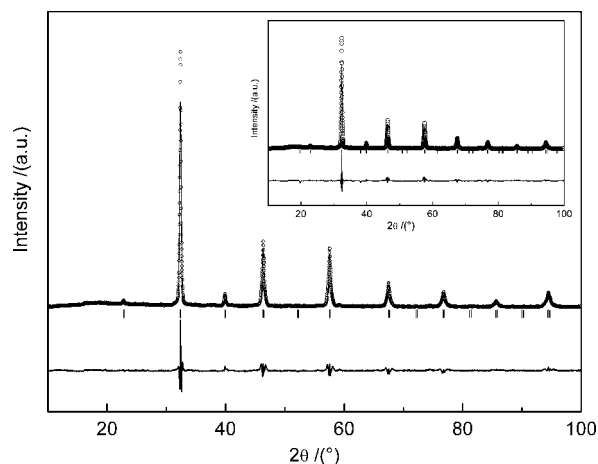


Figure 2. Rietveld refinement of the structure of Sr₄Fe₃ReO₁₂ from powder XRD data. Observed (○), calculated (—), and difference profiles (bottom) are shown. Vertical bars indicate positions of Bragg reflections. Inset shows refinement for the double perovskite (*Fm* $\bar{3}$ *m*) structure model, and the panel image shows refinement for the primitive cubic (*Pm* $\bar{3}$ *m*) perovskite structure model.

XRD data of Sr₄Co₃ReO₁₂ could be refined (Figure 1) on the basis of the double perovskite structure model¹⁴ (*Fm* $\bar{3}$ *m*), where the 4*a* sites are exclusively occupied by Co and the 4*b* sites are randomly occupied by Co_{0.5}Re_{0.5}; accordingly, we formulated the oxide as Sr₂(Co)_{4*a*}(Co_{0.5}Re_{0.5})_{4*b*}O₆. A similar double perovskite structure (*I4/m*) was reported¹⁵ for Sr₃Fe₂MoO₉ \equiv Sr₂(Fe)_{2*b*}(Fe_{1/3}Mo_{2/3})_{2*a*}O₆, where the 2*b* site is exclusively occupied by Fe³⁺ and the 2*a* site is occupied randomly by a mixture of 1/3Fe³⁺ and 2/3Mo⁶⁺.

The structural parameters derived from the refinement of Sr₄Co₃ReO₁₂ (Table 1) revealed that while the Co³⁺ atom at the 4*a* site is considerably overbonded [bond valence sum (BVS) for Co at 4*a* is 3.91; expected BVS is 3], the Co³⁺/Re⁷⁺ atoms at the 4*b* sites are significantly underbonded (BVS for Co/Re at 4*b* is 3.15; expected BVS is 5.0). Accordingly, the Co–O and Co/Re–O bond distances are

(11) Lasocha, W.; Lewinski, K. *J. Appl. Crystallogr.* **1994**, *27*, 437.

(12) Kraus, W.; Nolze, G. *J. Appl. Crystallogr.* **1996**, *29*, 301.

(13) Larson, A. C.; von Dreele, R. B. *General Structure Analysis System Report LAUR 86-748*; Los Alamos National Laboratory: Los Alamos, NM, 1990.

(14) Azad, A. K.; Ivanov, S. A.; Eriksson, S.-G.; Eriksen, J.; Rundlöf, H.; Mathieu, R.; Svedlindh, P. *Mater. Res. Bull.* **2001**, *36*, 2215.

(15) Viola, M. C.; Alonso, J. A.; Pedregosa, J. C.; Carbonio, R. E. *Eur. J. Inorg. Chem.* **2005**, 1559.

Table 1. Atomic Positions, Occupancy, and Isotropic Temperature Factors for Sr₄Co₃ReO₁₂^a

atom	Wyckoff position	x	y	z	B _{iso} (Å ²)	occupancy
Sr	8c	0.25	0.25	0.25	0.0241(4)	1.0
Co1	4a	0	0	0	0.0251(8)	1.0
Co2/Re	4b	0.5	0.5	0.5	0.0374(5)	0.5/0.5
O	24e	0.2352(4)	0	0	0.0419(9)	1.0

^a Space group $Fm\bar{3}m$, $a = 7.8153(2)$ Å. Reliability factors (%): $R_p = 1.02$, $R_{wp} = 1.79$, $R_F^2 = 4.16$, $\chi^2 = 8.953$. Bond lengths (Å): Sr–O = $2.7654(3) \times 12$, Co(1)–O = $1.8384(3) \times 6$, Co(2)/Re–O = $2.0691(3) \times 6$. Bond angles (deg): Co(1)–O–Co(2)/Re = 179.97 . Bond valence sums: Sr = 2.088, Co(1) = 3.912, Co(2)/Re = 3.147.

Table 2. Atomic Positions, Occupancy, and Isotropic Temperature Factors for Sr₄Fe₃ReO₁₂^a

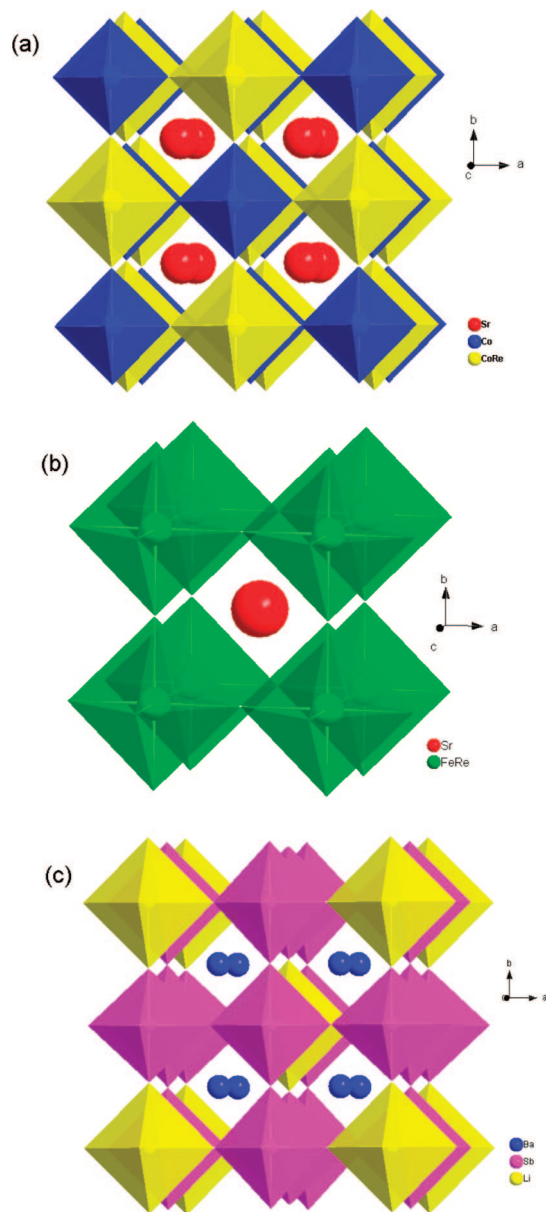
atom	Wyckoff position	x	y	z	B _{iso} (Å ²)	occupancy
Sr	1b	0.5	0.5	0.5	0.0367(7)	1.0
Fe/Re	1a	0	0	0	0.0296(6)	0.75/0.25
O	3d	0.5	0	0	0.0363(6)	1.0

^a Space group $Pm\bar{3}m$, $a = 3.9353(3)$ Å. Reliability factors (%): $R_p = 1.99$, $R_{wp} = 3.39$, $R_F^2 = 9.71$, $\chi^2 = 12.04$. Bond lengths (Å): Sr–O = $2.7827(3) \times 12$, Fe/Re–O = $1.9676(7) \times 6$. Bond angles (deg): Fe/Re–O–Fe/Re = 180 . Bond valence sums: Sr = 1.992, Fe/Re = 3.918. Rietveld refinement on the basis of the double perovskite structure ($Fm\bar{3}m$) model gave the following parameters: $a = 7.8697(3)$ Å, R_p (%) = 2.30, R_{wp} (%) = 3.96, R_F^2 (%) = 12.66, $\chi^2 = 16.42$.

shorter (1.84 Å) and longer (2.07 Å) than the values expected (2.01 and 1.97 Å) on the basis of Shannon¹⁶ ionic radii sums for the formal oxidation states of Co³⁺ (high spin) and Re⁷⁺. These results suggest the possibility of an electronic interaction between Co³⁺ and Re⁷⁺ in the partially ordered perovskite structure that likely has a bearing on the electronic properties.

A₄M₃M'O₁₂ perovskite oxides are known to adopt ordered superstructures¹⁷ where the M site atoms are fully ordered; for example, Ba₄Sb₃LiO₁₂ has a 1:3 ordered superstructure ($Im\bar{3}m$) where Li occupies the center and vertices of the $2a_p$ unit cell and Sb occupies the center of the faces and middle of the edges.¹⁷ A similar but less symmetric ($P2_1/n$) superstructure was found for Sr₄Sb₃NaO₁₂.¹⁸ We attempted to refine the powder XRD data of Sr₄Co₃ReO₁₂ on the basis of the foregoing $Im\bar{3}m$ and $P2_1/n$ models but without any improvement over the double perovskite ($Fm\bar{3}m$) model.

Unlike the XRD pattern of Sr₄Co₃ReO₁₂, the pattern of the iron analogue, Sr₄Fe₃ReO₁₂ (Figure 2), does not show obvious superstructure reflections. We tried to refine the powder XRD data on the basis of both the primitive cubic perovskite structure ($Pm\bar{3}m$) as well as the double perovskite structure ($Fm\bar{3}m$) models. The refinement results (Figure 2) together with reliability factors (Table 2) seem to suggest that the refinement fit is better for the primitive perovskite ($Pm\bar{3}m$) model. Accordingly, we believe that the Fe and Re atoms in Sr₄Fe₃ReO₁₂ are not ordered in the long range, at least in the length scale of powder XRD measurements. Interestingly, the BVS for Fe/Re (3.92) in this oxide (Table 2) is not very much different from the ideal value (4.00), indicating that both Fe/Re on the average are not significantly

**Figure 3.** Crystal structure of (a) Sr₄Co₃ReO₁₂ and (b) Sr₄Fe₃ReO₁₂. In panel c, the structure of Ba₄Sb₃LiO₁₂ is shown.¹⁷

underbonded. Figure 3 shows the perovskite structures of Sr₄M₃ReO₁₂; for comparison, the fully ordered 1:3 structure of Ba₄Sb₃LiO₁₂ also is shown.

We investigated the magnetic and electrical properties of Sr₄M₃ReO₁₂ (M = Co, Fe). Our investigations revealed that both oxides are ferromagnetic semiconductors. Temperature dependence of magnetization measured at various fields (50 Oe to 1 T) (Figure 4) showed that the M = Co phase becomes ferromagnetic around 250 K. The Curie–Weiss plot of the data above 200 K yielded a positive Weiss constant ($\theta = 185$ K) and an effective magnetic moment ($\mu_{\text{eff}} = 2.6 \mu_B/\text{Co}$). The divergence of magnetization for the FC and ZFC measurements together with the downward drift of ZFC data at low temperatures showing a cusp over a broad temperature range of 200–50 K are clear signatures of a magnetically inhomogeneous (disordered) material.^{19–21} This result also is consistent with the partially disordered double perovskite structure of this material. The FC magnetization increases

(16) Shannon, R. D. *Acta Crystallogr., Sect. A: Found. Crystallogr.* **1976**, *32*, 751.

(17) Jacobson, A. J.; Collins, B. M.; Fender, B. E. F. *Acta Crystallogr., Sect. B: Struct. Sci.* **1974**, *30*, 1705.

(18) Alonso, J. A.; Mzayek, E.; Rasines, I. J. *Solid State Chem.* **1990**, *84*, 16.

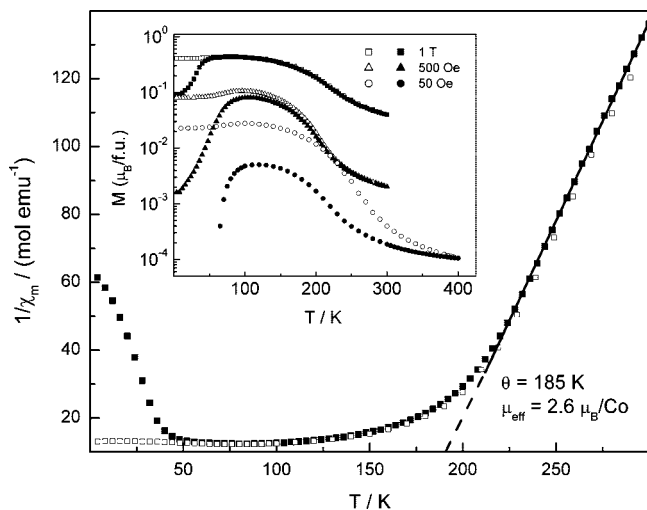


Figure 4. Inverse molar magnetic susceptibility ($1/\chi_m$) vs T plot for $\text{Sr}_4\text{Co}_3\text{ReO}_{12}$ under FC (\square) and ZFC (\blacksquare) conditions. Inset shows the temperature dependence of FC and ZFC magnetizations at different applied fields.

with increasing field but does not saturate even at 1 T. The highest magnetization observed at 1 T ($0.4 \mu_B$) suggests that the material is a bulk ferromagnet.

For an interpretation of the ferromagnetism of this material, we needed to know the exact oxidation and spin states of cobalt and rhenium. The formal oxidation states of cobalt and rhenium are 3+ and 7+, respectively, for the formula $\text{Sr}_4\text{Co}_3\text{ReO}_{12}$. Trivalent cobalt could exist in low spin (Co^{III} : t_{2g}^6 ; $S = 0$, nonmagnetic), high spin (Co^{3+} : t_{2g}^4 and e_g^2 ; $S = 2$), and intermediate spin (Co^{III} : t_{2g}^5 and e_g^1 ; $S = 1$) states, of which the magnetic interaction ($\text{Co}^{3+}-\text{O}-\text{Co}^{3+}$) between high spin cobalt in the perovskite structure is expected to be antiferromagnetic, while the interaction between the Jahn–Teller active intermediate spin cobalt ($\text{Co}^{\text{III}}-\text{O}-\text{Co}^{\text{III}}$) could give rise to ferromagnetic coupling as observed for LaCoO_3 .^{22,23} But, the T_c for this interaction is rather low ($T_c = \sim 85$ K), and the experimental T_c value >185 K observed for $\text{Sr}_4\text{Co}_3\text{ReO}_{12}$ suggests that it may not be entirely due to this interaction; the paramagnetic μ_{eff} of $2.6 \mu_B$ is, however, fairly close to the ideal μ_{eff} ($2.83 \mu_B$) expected for the intermediate spin Co^{III} ($S = 1$) state. Accordingly, ferromagnetism of these oxides would be caused by the electronic interaction between intermediate spin $\text{Co}^{\text{III}}-\text{O}-\text{Re}^{\text{VII}}$. Considering that the magnetic interaction in double perovskites, $\text{A}_2\text{MM}'\text{O}_6$, exhibiting high T_c invariably involves electron hopping between M and M' atoms that produces mixed valences (i.e., $\text{Fe}^{2+/3+}-\text{O}-\text{Mo}^{6+/5+}$ in $\text{Sr}_2\text{FeMoO}_6$) and also that an electronic interaction between integral valence $\text{Co}^{\text{III}}(3d^6)-\text{O}-\text{Re}^{\text{VII}}(5d^0)$ is not likely to produce ferromagnetism, we believe that the electronic interaction between Co^{III} and Re^{VII} in $\text{Sr}_4\text{Co}_3\text{ReO}_{12}$ involves mixed

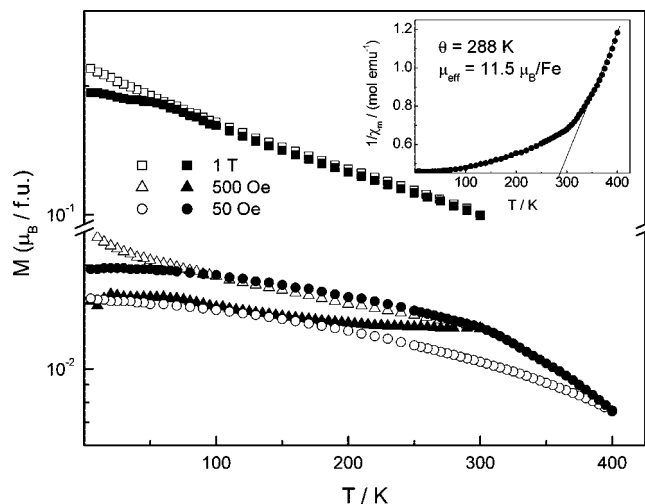


Figure 5. Temperature dependence of FC (open symbols) and ZFC (solid symbols) magnetizations for $\text{Sr}_4\text{Fe}_3\text{ReO}_{12}$ at different applied fields. Inset shows a plot of inverse molar magnetic susceptibility ($1/\chi_m$) vs T at 50 Oe.

valence states, $\text{Co}^{\text{III/IV}}-\text{O}-\text{Re}^{\text{VII/VI}}$, in a manner similar to the electronic interaction¹ in $\text{Sr}_2\text{FeMoO}_6$ and $\text{Sr}_2\text{FeReO}_6$, resulting in the observed high temperature ferromagnetism.

Further support for this mechanism comes from the magnetic properties of $\text{Sr}_4\text{Fe}_3\text{ReO}_{12}$. Magnetization studies (Figure 5) show a clear ferromagnetism around room temperature that does not saturate even at 1 T (the magnetization at 1 T is $0.22 \mu_B/\text{f.u.}$). The Curie–Weiss plot (Figure 5 inset) above 300 K shows a linear region with a positive Weiss constant of ~ 290 K, providing further support to the ferromagnetic interaction. The μ_{eff} obtained from the Curie–Weiss plot ($11.5 \mu_B/\text{Fe}$) is, however, much larger than the value expected ($5.92 \mu_B$) for the Fe^{3+} : $t_{2g}^3 e_g^2$ ($S = 5/2$) state. Inasmuch as the magnetic interaction $\text{Fe}^{3+}(t_{2g}^3 e_g^2)-\text{O}-\text{Fe}^{3+}(t_{2g}^3 e_g^2)$ in the perovskite structure would only be antiferromagnetic, the observed ferromagnetic property of $\text{Sr}_4\text{Fe}_3\text{ReO}_{12}$ would arise from the $\text{Fe}-\text{O}-\text{Re}$ interaction that likely involves mixed valence states, $\text{Fe}^{3+/4+}-\text{O}-\text{Re}^{7+/6+}$, similar to $\text{Sr}_4\text{Co}_3\text{ReO}_{12}$ discussed previously.

$M-H$ hysteresis loops (Figure 6) provide further support for the occurrence of bulk ferromagnetism in both $\text{Sr}_4\text{M}_3\text{ReO}_{12}$ compounds ($M = \text{Co}, \text{Fe}$). The magnetic parameters derived from the hysteresis data are listed in Table 3; the values are similar to other bulk ferromagnetic oxide materials.¹⁹ Characteristically, both coercivity (H_c) and remanence (M_r) decrease with increasing temperature, and the loops almost vanish at higher temperatures. This behavior seems to suggest that the materials pass into a superparamagnetic state at higher temperatures where the observed magnetism is due to small magnetic clusters/islands whose moments are randomly oriented. This picture also is consistent with the large paramagnetic μ_{eff} observed for $\text{Sr}_4\text{Fe}_3\text{ReO}_{12}$ (Figure 5).

The dc electrical resistivity measurement (Figure 7) shows that both $\text{Sr}_4\text{M}_3\text{ReO}_{12}$ compounds are semiconductors with the temperature variation of the resistivity being more Arrhenius-like for the $M = \text{Fe}$ phase; the data for the $M = \text{Co}$ phase seem to obey a variable range hopping (VRH)

(19) Dass, R. I.; Goodenough, J. B. *Phys. Rev. B: Condens. Matter Mater. Phys.* **2003**, *67*, 14401.

(20) He, T.; Cava, R. J. *Phys. Rev. B: Condens. Matter Mater. Phys.* **2001**, *63*, 172403.

(21) He, T.; Cava, R. J. *J. Phys.: Condens. Matter* **2001**, *13*, 8347.

(22) Yan, J.-Q.; Zhou, J. -S.; Goodenough, J. B. *Phys. Rev. B: Condens. Matter Mater. Phys.* **2004**, *70*, 14402.

(23) Zhou, S.; Shi, L.; Zhao, J.; He, L.; Yang, H.; Zhang, S. *Phys. Rev. B: Condens. Matter Mater. Phys.* **2007**, *76*, 172407.

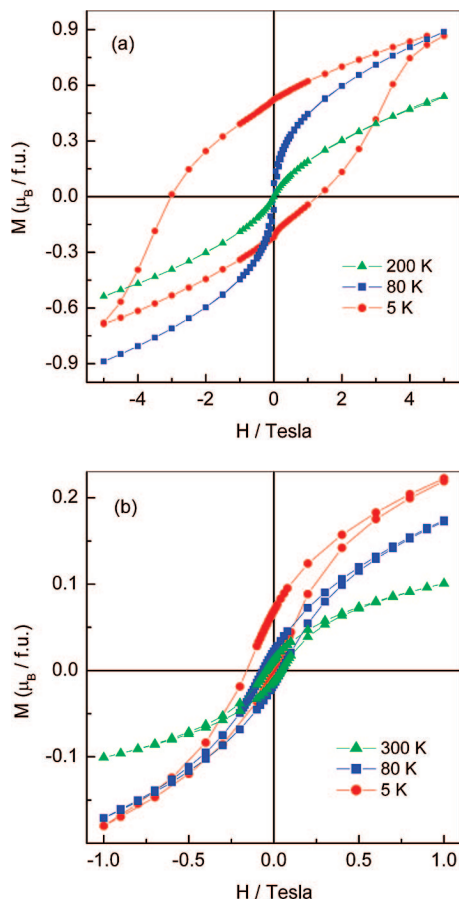


Figure 6. M – H hysteresis loops for (a) $\text{Sr}_4\text{Co}_3\text{ReO}_{12}$ and (b) $\text{Sr}_4\text{Fe}_3\text{ReO}_{12}$ at different temperatures under FC conditions ($H_{\text{FC}} = 1$ T).

Table 3. Magnetic Properties of $\text{Sr}_4\text{M}_3\text{ReO}_{12}$ ($\text{M} = \text{Co}, \text{Fe}$)^a

sample	M_s (5 K, 1 T) ($\mu_B/\text{f.u.}$)	M_r (5 K) ($\mu_B/\text{f.u.}$)	H_c (5 K) (T)	μ_{eff} (μ_B)	θ (K)
$\text{Sr}_4\text{Co}_3\text{ReO}_{12}$	0.41	0.37	2.17	2.6/Co	185
$\text{Sr}_4\text{Fe}_3\text{ReO}_{12}$	0.22	0.03	0.08	11.5/Fe	288

^a M_s (1 T), M_r , and H_c are saturation magnetization at 1 T, remanent magnetization, and coercivity, respectively.

model,^{24,25} showing a linear $\ln(\rho)$ versus $T^{-1/4}$ dependence. Interestingly, the $\text{M} = \text{Co}$ phase has a significantly lower resistivity at room temperature than the $\text{M} = \text{Fe}$ phase, which is consistent with the lower energy expected for the electron transfer $\text{Co}^{3+} + \text{Re}^{7+} \leftrightarrow \text{Co}^{4+} + \text{Re}^{6+}$ than that for the transfer $\text{Fe}^{3+} + \text{Re}^{7+} \leftrightarrow \text{Fe}^{4+} + \text{Re}^{6+}$ (ref 2).

We identified two new magnetic interactions, $\text{M}^{3+/4+}-\text{O}-\text{Re}^{7+/6+}$ ($\text{M} = \text{Co}, \text{Fe}$) that gave rise to high temperature ferromagnetism in perovskite oxides $\text{Sr}_4\text{M}_3\text{ReO}_{12}$. While the $\text{M} = \text{Co}$ phase adopted a partially ordered double perovskite structure ($Fm\bar{3}m$; $a = 7.8153$ Å), $\text{Sr}_2\text{Co}[\text{Co}_{0.5}\text{Re}_{0.5}]\text{O}_6$, the $\text{M} = \text{Fe}$ phase exhibited a primitive cubic perovskite structure

(24) Mott, N. F.; Davis, E. A. *Electronic Processes in Non-Crystalline Materials*; Clarendon Press: Oxford, 1971.

(25) Snyder, G. J.; Booth, C. H.; Bridges, F.; Hiskes, R.; DiCarolis, S.; Beasley, M. R.; Geballe, T. H. *Phys. Rev. B: Condens. Matter Mater. Phys.* **1997**, *55*, 6453.

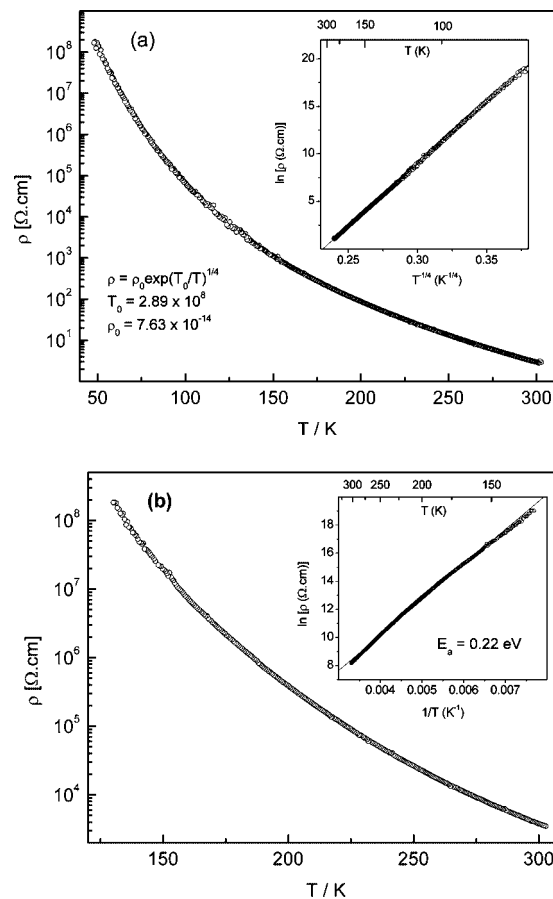


Figure 7. Variation of dc electrical resistivity with temperature for (a) $\text{Sr}_4\text{Co}_3\text{ReO}_{12}$ and (b) $\text{Sr}_4\text{Fe}_3\text{ReO}_{12}$. Insets show VRH fit and Arrhenius fit of the resistivity data for panels a and b, respectively.

($Pm\bar{3}m$; $a = 3.9353$ Å) wherein the transition metal atoms were disordered at the octahedral sites. The ferromagnetism most likely arises from a magnetic interaction, $\text{M}^{3+/4+}-\text{O}-\text{Re}^{7+/6+}$, that involves mixed valence states for both $\text{M} = \text{Co}$ and Fe as well as Re , but the disordered distribution of M and Re atoms in the perovskite structure precludes a long-range magnetic order and a definite ferromagnetic ordering temperature T_c for both materials. Clearly, further work is needed to identify the mixed valence states of the transition metals and the nature of magnetic interaction that cause high temperature ferromagnetism in these materials.

Acknowledgment. We thank the Department of Science and Technology, Government of India, for support of this research work through a Ramanna Fellowship and research project (SR/S1/PC-14/2002).

Supporting Information Available: TG curves for hydrogen reduction of $\text{Sr}_4\text{M}_3\text{ReO}_{12}$ ($\text{M} = \text{Co}, \text{Fe}$) (Figure S1) and SEM image $\text{Sr}_4\text{Co}_3\text{ReO}_{12}$ (Figure S2). This material is available free of charge via the Internet at <http://pubs.acs.org>.

CM800749S